JOURNAL OF SOLID STATE CHEMISTRY **24**, 41–55 (1978)

Order–Disorder Transition of the Metal Vacancies in the Vanadium–Sulfur System II. A Statistical Thermodynamic Treatment

Y. OKA, K. KOSUGE, AND S. KACHI

Department of Chemistry, Faculty of Science, Kyoto University, Kyoto, Japan

Received July 18, 1977; in revised form September 2, 1977

A statistical thermodynamic treatment is made on the problem of the order–disorder transition of metal vacancies in the V–S system. The total free energy (*G*) for the crystal with interacting defects is expressed after Libowitz and Lightstone based on the Bragg–Williams approximation. From the calculation, two types of transitions are derived corresponding to $V_5S_8 \leftrightarrow V_3S_4$ (at Tc_2) and $V_3S_4 \leftrightarrow CdI_2$ (at Tc_1) and they are of second order, which is consistent with our previous experimental work. The calculated phase diagram is compared with the experimental one for the V–S system and also for the V–Se system. Equilibrium sulfur vapor pressure is also calculated from the total free energy (*G*) and the results are compared with the experimental data of Wakihara, Uchida, and Taniguchi (*Mater. Res. Bull.* **11**, 973 (1976)).

1. Introduction

On the nature of point defects (random distribution) in inorganic compounds, many thermodynamic treatments have been made from which we can deduce the stability range and the equilibrium vapor pressure of nonstoichiometric compounds. In the case of noninteracting point defects (low concentration of defects), the treatment is very simple as was shown by Libowitz (*1*). With an increasing number of defects, the interaction between defects must be taken into consideration. The most simplified treatment on the interaction energy between defects has been made by Lightstone and Libowitz (L and L) (*2*), by use of the Bragg–Williams approximation which has been recognized to be successful for the order–disorder transition of alloys. For the problems on ordered structures of point defects, few papers have been published so far. Koiwa and Hirabayashi (*3*) have studied the order–disorder transformation of oxygen atoms in the Ti–O system, in which oxygen atoms dissolve interstitially in an alpha-titanium matrix. They expressed the free energy for this system in terms of the pairwise interaction energies between oxygen atoms and the configurational entropy of interstitial oxygen atoms on the basis of the Bragg–Williams approximation. But their expression does not give the total free energy of the system, which will be shown later. L and L (*2*) derived theoretically the relation between the concentration of defects and the activity of the volatile elements in the nonstoichiometric compounds, assuming that one type of point defect was predominant. They used the Bragg–Williams approximation for the system with interacting point defects. Their expression of the free energy consists of four sets of terms, i.e., the free energy of the ideal perfect crystal

0022-4596/78/0241-0041$02.00/0

Printed in Great Britain

from which the real crystal is derived, the free energy change for introducing the point defects, the free energy of interaction between the point defects, and the configurational entropy. The total free energy gives the absolute values of the free energy of the system over the whole range of composition.

In the previous paper (*4*), the present authors have clarified experimentally the order–disorder transitions of the metal vacancies in the V–S and V–Se system. In these systems, the vacancy-ordered V_5S_8-type transforms into the vacancy-ordered V_3S_4-type structure at Tc_2, which can be regarded as the disordering of the V_5S_8-type structure, and finally into the nonstoichiometric CdI_2-type structure (intralayer disorder) at Tc_1. This paper presents the statistical thermodynamic treatment of the V–S and V–Se systems, by making use of the modified free energy expression proposed by L and L.

2. Model and Free Energy

2.1 Model

In the pseudobinary VS–VS_2 system, four phases appear with increasing temperature or sulfur content, i.e., NiAs, V_3S_4, V_5S_8, and CdI_2-type structures (*5–7*). For example, the sample $VS_{1.60}$ shows the following transformations with increasing temperature; V_5S_8-type $\xrightarrow{Tc_2}$ V_3S_4-type $\xrightarrow{Tc_1}$ CdI_2-type $\xrightarrow{?}$ (NiAs-type). The transformations at Tc_1 and Tc_2 may be second order. At room temperature, the samples quenched from 800°C show successive phase transition VS-type (NiAs) → V_3S_4-type → V_5S_8-type → CdI_2-type with increasing sulfur content (*5*). We mention here the structure model, which includes all the structures appearing in the V–S system.

The V_5S_8-type structure can be taken as a basic structure. The structure of the V_5S_8-type is shown in Fig. 1 (*8*, *9*), where sulfur atoms are omitted for simplicity. The characteristic of the structure is the alternate stacking of a partially occupied metal layer and a fully occupied one along the *c*-axis.

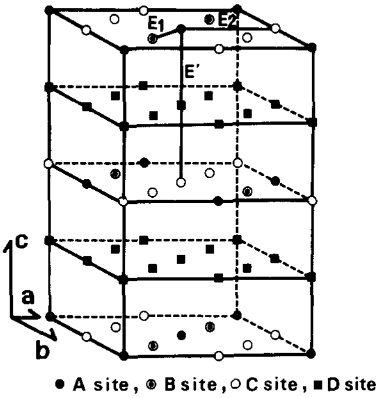

FIG. 1. Crystal structure of the V_5S_8-type. For simplicity only metal sites are shown, which are classified into four kinds, i.e., A, B, C, and D sites. E_1 is the nearest-neighbor interaction energy of vacancy pairs in a metal layer, i.e., A–B, B–C, C–A, and C–C pairs, and A–B pair is shown in the figure for an example. E_2 is the second-nearest-neighbor one, i.e., A–B, B–C, C–A, and C–C pairs. E′ is the interaction energy between vacancies in alternate layers through D site, i.e., A–C and B–C pairs. It is to be noted that the interaction energy depends only on the distance between vacancies.

The sites of metal atoms can be classified into four sublattice sites A, B, C, and D, as shown in Fig. 1.[1] When the occupation probabilities for A, B, C, and D sites are expressed by *a*, *b*, *c*, and *d*, respectively, each structure type with the stoichiometric composition at 0°K can be defined as follows:

	Type	
$a = b = c = d = 1$	NiAs	$(VS_{1.00})$
$a = b = c = 0, d = 1$	CdI_2	$(VS_{2.00})$
$a = b = 1, c = 0, d = 1$	V_3S_4	$(VS_{1.33})$
$a = 1, b = c = 0, d = 1$	V_5S_8	$(VS_{1.60})$

---

[1] Strictly speaking, the D site should be classified crystallographically into two kinds of sites, D_1 and D_2. Along the direction of the *c*-axis the D_1 site has A and C sites as the nearest neighbors, and the D_2 site has B and C sites. This classification is the same as the result of the NMR study (*10*, *11*), i.e., D_1 site corresponds to site II and D_2 site to site III in Ref. (*10*). Our calculation is based on the assumption that a fully occupied layer is uniform and has no vacancy. The assumption is justified by the fact that a recent study on the determination of the crystal structure V_5S_8 by Kawada *et al.* (*9*) revealed that a fully occupied layer has no vacancy within experimental error.

For nonstoichiometric composition or at finite temperature, the above mentioned relations have to be altered as follows:

	Type
$a = b = c = d < 1$	NiAs
$a = b = c < 1, d \simeq 1$	CdI_2
$a = b > c, d \simeq 1$	V_3S_4
$a > b \geq c, d \simeq 1$	V_5S_8

The structural transformations in the V–S system can be realized by the temperature or composition dependence of the occupation probabilities a, b, c, and d. For example, the transition from the V_5S_8-type to the V_3S_4-type structure corresponds to the change from $a > b \geq c$ to $a = b > c$, and the transition from the V_3S_4-type to the CdI_2-type corresponds to that from $a = b > c$ to $a = b = c$. In the following section, the total free energy of the system will be calculated on the basis of this model.

2.2 Free Energy

In order to discuss the nature of the phase transition, it is necessary to give the total free energy (G) of the system. The present treatment is based on the calculation of free energy proposed by L and L (*2*).

The total free energy may be written as

$$G = G(N, N_S, N_A, N_B, N_C, N_D),$$

where N is the number of metal sites (equal to the number of anion sites in this case), N_S is the number of sulfur atoms, N_A, N_B, N_C, and N_D are the number of metal atoms on A, B, C, and D sites, respectively. From the definition of metal sites, the number of A, B, C, and D sites is $\frac{1}{8}N$, $\frac{1}{8}N$, $\frac{1}{4}N$, and $\frac{1}{2}N$, respectively. Accordingly, the occupation probabilities a, b, c, and d can be given as follows;

$$a = N_A/N/8, \quad b = N_B/N/8, \quad c = N_C/N/4 \quad \text{and} \quad d = N_D/N/2.$$

For simplicity, we make a plausible assumption that there is no vacancy in the fully occupied layer, i.e., $N_D = N/2$, because our treatment is centered on the *intralayer* structural transformation.

We here outline the basic framework of the constituents of the total free energy (G) after L and L. We start from the ideal crystal $VS_{1.00}$ (without imperfection). The real crystal is derived by introducing vacancies into this ideal crystal. The expression of the total free energy consists of four sets of terms:

(i) Free energy of the ideal crystal $N\mu_{VS}$,

(ii) Free energy change for introducing vacancies.

(iii) Free energy of interaction between vacancies. The interaction energy was calculated by use of the Bragg–Williams approximation. As for metal vacancies, the interaction energy between vacancy–vacancy and metal–vacancy must be taken into consideration in principle. As will be discussed in Section 4, it can be proved that the expression including only vacancy–vacancy interaction gives the same result on the nature of the phase transition as the expression including vacancy–vacancy and metal–vacancy interaction does. In this paper, only the interaction energy between vacancy–vacancy (see Fig. 1) is taken into consideration for simplicity. It is to be noted that the interaction energy between metal–metal is included in the term $N\mu_{VS}$.

(iv) Configurational entropy of vanadium atoms and sulfur atoms.

The total free energy is given as follows;

$$\begin{aligned} G = {} & N\mu_{VS} + (N - N_S)g_S \\ & + \left(\frac{N}{2} - N_A - N_B - N_C\right) g_V \\ & + \frac{z_S}{2}\frac{(N - N_S)^2}{N}\xi_S \\ & + \left[\frac{1}{2}\left(\frac{N}{8} - N_A\right)\left\{2\left(\frac{N}{8} - N_B\right)\Big/\frac{N}{8}\right.\right. \\ & \left.\left. + 4\left(\frac{N}{4} - N_C\right)\Big/\frac{N}{4}\right\} + \frac{1}{2}\left(\frac{N}{8} - N_B\right)\right. \\ & \left.\left\{2\left(\frac{N}{8} - N_A\right)\Big/\frac{N}{8} + 4\left(\frac{N}{4} - N_C\right)\Big/\frac{N}{4}\right\}\right. \end{aligned}$$

$$+ \frac{1}{2}\left(\frac{N}{4} - N_C\right)\left\{2\left(\frac{N}{8} - N_A\right)\Big/\frac{N}{8} + 2\left(\frac{N}{8} - N_B\right)\Big/\frac{N}{8} + 2\left(\frac{N}{4} - N_C\right)\Big/\frac{N}{4}\right\}\Bigg](E_1 + E_2)$$

$$+ \left[\left(\frac{N}{8} - N_A\right)\left(\frac{N}{4} - N_C\right)\Big/\frac{N}{4} + \left(\frac{N}{8} - N_B\right)\left(\frac{N}{4} - N_C\right)\Big/\frac{N}{4} + \frac{1}{2}\left(\frac{N}{4} - N_C\right)\left\{\left(\frac{N}{8} - N_A\right)\Big/\frac{N}{8} + \left(\frac{N}{8} - N_B\right)\Big/\frac{N}{8}\right\}\right]E'$$

$$+ kT \ln \frac{N!}{(N - N_S)!N_S!} \cdot \frac{\left(\frac{N}{8}\right)!}{\left(\frac{N}{8} - N_A\right)!N_A!} \cdot \frac{\left(\frac{N}{8}\right)!}{\left(\frac{N}{8} - N_B\right)!N_B!} \cdot \frac{\left(\frac{N}{4}\right)!}{\left(\frac{N}{4} - N_C\right)!N_C!} \qquad (1)$$

where g_S and g_V are the vacancy formation energies for sulfur and vanadium atoms, respectively. ζ_S is the interaction energy between sulfur vacancies; z_S is the coordination number of sulfur atoms. E_1 is the nearest-neighbor interaction energy of vanadium vacancy pairs in a metal layer, i.e., A–B, B–C, C–A, and C–C pairs, and E_2 is the second-nearest-neighbor one of vacancy pairs, i.e., A–B, B–C, C–A, and C–C pairs. E' is the interlayer interaction energy of vacancy pairs through D site, i.e., A–C and B–C pairs (see Fig. 1). In the real crystal of the V_5S_8-type, the array of metal sites in the same layer is slightly distorted from the ideal hexagonal. In this paper, the calculation was made on the assumption that every metal site is surrounded by six metal sites in the regular hexagonal array.

Equation (1) can be reduced to the following expression:

$$\begin{aligned}
G = {} & N\mu_{VS} \\
& + (N - N_S)g_S \\
& + \left(\frac{N}{2} - N_A - N_B - N_C\right) g_V \\
& + \frac{z_S}{2}\frac{(N - N_S)^2}{N}\zeta_S \\
& + \left\{\frac{3}{2}N - 6(N_A + N_B + N_C)\right. \\
& \left. + \frac{4}{N}\left(4N_A N_B + 4N_A N_C + 4N_B N_C + N_C^2\right)\right\}\zeta \\
& + \left\{\frac{N}{2} - 2(N_A + N_B + N_C)\right. \\
& \left. + \frac{8}{N}N_C(N_A + N_B)\right\}\zeta_V' \\
& + kT\left\{(N - N_S)\ln(N - N_S)\right. \\
& + N_S \ln N_S + \left(\frac{N}{8} - N_A\right) \ln\left(\frac{N}{8} - N_A\right) \\
& + N_A \ln N_A \left(\frac{N}{8} - N_B\right) \ln\left(\frac{N}{8} - N_B\right) \\
& + N_B \ln N_B + \left(\frac{N}{4} - N_C\right) \ln\left(\frac{N}{4} - N_C\right) \\
& \left. + N_C \ln N_C - \frac{3}{2}N\ln N + \frac{5}{4}N\ln 2\right\} \qquad (2)
\end{aligned}$$

where $\zeta_V = E_1 + E_2$ and $\zeta_V' = E'$.

2.3. *Chemical Equilibrium*

At chemical equilibrium, the following condition has to hold:

$$(\partial G/\partial N)\ N_S, N_A, N_B, N_C = 0. \tag{3}$$

Therefore:

$$\mu_{VS} + g_S + \frac{1}{2}g_V + \frac{z_S}{2}\left(1 - \frac{N_S^2}{N^2}\right)\xi_S + \left\{\frac{3}{2} - \frac{4}{N^2}(4N_AN_B + 4N_AN_C + 4N_BN_C + N_C{}^2)\right\}\xi_V + \left\{\frac{1}{2} - \frac{8}{N^2}N_C(N_A + N_B)\right\}\xi'_V + kT\left\{\ln(N - N_S) + \frac{1}{8}\ln\left(\frac{N}{8} - N_A\right) + \frac{1}{8}\ln\left(\frac{N}{8} - N_B\right) + \frac{1}{4}\ln\left(\frac{N}{4} - N_C\right) - \frac{3}{2}N\ln N + \frac{5}{4}N\ln 2\right\} = 0. \tag{4}$$

The chemical potentials of every site can be given as the derivative of the total free energy G. We have:

$$\mu_S = \frac{\partial G}{\partial N_S} = -g_S - z_S\left(\frac{N - N_S}{N}\right)\xi_S + kT\left\{\ln N_S - \ln(N - N_S)\right\}, \tag{5}$$

$$\mu_V^A = \frac{\partial G}{\partial N_A} = -g_V + \left\{-6 + \frac{16}{N}(N_B + N_C)\right\}\xi_V + \left(-2 + \frac{8N_C}{N}\right)\xi'_V + kT\left\{\ln N_A - \ln\left(\frac{N}{8} - N_A\right)\right\}, \tag{6}$$

$$\mu_V^B = \frac{\partial G}{\partial N_B} = -g_V + \left\{-6 + \frac{16}{N}(N_A + N_C)\right\}\xi_V + \left(-2 + \frac{8N_C}{N}\right)\xi'_V + kT\left\{\ln N_B - \ln\left(\frac{N}{8} - N_B\right)\right\}, \tag{7}$$

$$\mu_V^C = \frac{\partial G}{\partial N_C} = -g_V + \left\{-6 + \frac{8}{N}(2N_A + 2N_B + N_C)\right\}\xi_V + \left\{-2 + \frac{8(N_A + N_B)}{N}\right\}\xi'_V + kT\left\{\ln N_C - \ln\left(\frac{N}{4} - N_C\right)\right\}, \tag{8}$$

where μ_S is the chemical potential of sulfur atoms and μ_V^A, μ_V^B, and μ_V^C are the chemical potentials of vanadium atoms on A, B, and C sites, respectively.

From the internal equilibrium condition, we have:

$$\mu_V^A = \mu_V^B = \mu_V^C = \mu_V, \tag{9}$$

where μ_V is the chemical potential of vanadium atoms in the crystal. From Eq. (9) the following equations can be given:

$$\mu_V^A - \mu_V^C = 0, \tag{10}$$

$$\mu_V^B - \mu_V^C = 0. \tag{11}$$

Using Eqs. (6), (7), and (8), Eqs. (10) and (11) yield:

$$\frac{8}{N}(N_C - 2N_A)\xi_V + \frac{8}{N}(N_C - N_A - N_B)\xi'_V + kT \ln N_A\left(\frac{N}{4} - N_C\right) \Big/ \left(\frac{N}{8} - N_A\right)N_C = 0, \tag{12}$$

$$\frac{8}{N}(N_C - 2N_B)\xi_V + \frac{8}{N}(N_C - N_A - N_B)\xi'_V + kT \ln N_B\left(\frac{N}{4} - N_C\right) \Big/ \left(\frac{N}{8} - N_B\right)N_C = 0. \tag{13}$$

We hereafter use the occupation probabilities a, b, and c instead of the number of vanadium atoms. Equations (12), and (13) lead to the following equations:

$$2(c - a)\xi_V + (2c - a - b)\xi'_V + kT \ln \frac{a(1 - c)}{(1 - a)c} = 0, \tag{14}$$

$$2(c - b)\xi_V + (2c - a - b)\xi'_V + kT \ln \frac{b(1 - c)}{(1 - b)c} = 0. \tag{15}$$

These equations give the temperature and composition dependence of the occupation probabilities at equilibrium. Under the condition of fixed number of vanadium atoms, namely $a + b + 2c = x$ (x: constant) and replacing ξ'_V and kT with $\alpha\xi_V$ and $t\xi_V$, respectively, we get:

$$(x - 3a - b) + \alpha(x - 2a - 2b) + t \ln \frac{a(2 - x + a + b)}{(1 - a)(x - a - b)} = 0, \tag{16}$$

$$(x - a - 3b) + \alpha(x - 2a - 2b) + t \ln \frac{b(2 - x + a + b)}{(1 - b)(x - a - b)} = 0, \tag{17}$$

Under the assumption that the number of sulfur vacancies is negligible, the ratio of sulfur and vanadium atoms X in VS_X may be expressed:

$$X = \frac{N}{\frac{N}{2} + N_A + N_B + N_C} = \frac{8}{4 + a + b + 2c} = \frac{8}{4 + x}. \tag{18}$$

By setting the values of α, t, and x, Eqs. (16) and (17) were solved numerically under the condition of the free energy minimum, using a computer (FACOM 230–75, Kyoto University).

2.4. *Equilibrium Sulfur Vapor Pressure*

The chemical potential of sulfur atoms in the solid is expressed in terms of the sulfur activity (a_S) by the following equation:

$$\mu_S = kT \ln a_S. \tag{19}$$

At chemical equilibrium, μ_S is equal to that in the gas phase:

$$\mu_S = \tfrac{1}{2}\mu_{S_2}(g) = \tfrac{1}{2}\mu^0_{S_2}(g) + \tfrac{1}{2}kT \ln P_{S_2}, \tag{20}$$

where $\mu_{S_2}(g)$ is the chemical potential of sulfur molecules (S_2), $\mu^0_{S_2}(g)$ is that in the standard state, and P_{S_2} is the equilibrium sulfur vapor pressure. If we choose one atmosphere as the standard state of the sulfur vapor pressure, P_{S_2} is given from Eq. (20):

$$P_{S_2} = \tfrac{1}{2} \exp(\mu_S/kT). \tag{21}$$

By eliminating g_S from Eqs. (4) and (5), we obtain:

$$\mu_S = \mu_{VS} + \frac{1}{2}g_V - 3\left(1 - \frac{N_S}{N}\right)^2 \xi_S + \left\{\frac{3}{2} - \frac{4}{N^2}(4N_A N_B + 4N_A N_C + 4N_B N_C\right.$$

$$+ N_C^2)\Big\}\xi_V + \Big\{\frac{1}{2} - \frac{8}{N^2}N_C(N_A$$

$$+ N_B)\Big\}\xi_V + kT\Big\{\ln N_S$$

$$+ \frac{1}{8}\ln\left(\frac{N}{8} - N_A\right) + \frac{1}{8}\ln\left(\frac{N}{8} - N_B\right)$$

$$+ \frac{1}{4}\ln\left(\frac{N}{4} - N_C\right) - \frac{3}{2}\ln N$$

$$+ \frac{5}{4}\ln 2\Big\}. \qquad (22)$$

In our case, we can assume the number of sulfur vacancies $(N - N_S)$ is negligibly small. From Eq. (21), we have:

$$\mu_S = \mu_{VS} + \frac{1}{2}g_V + \Big\{\frac{3}{2} - \frac{4}{N^2}(4N_AN_B$$

$$+ 4N_AN_C + 4N_BN_C + N_C^2)\Big\}\xi_V$$

$$+ \Big\{\frac{1}{2} - \frac{8}{N^2}N_C(N_A + N_B)\Big\}\xi_V$$

$$+ kT\Big\{\frac{1}{8}\ln\left(\frac{N}{8} - N_A\right)$$

$$+ \frac{1}{8}\ln\left(\frac{N}{8} - N_B\right)$$

$$+ \frac{1}{4}\ln\left(\frac{N}{4} - N_C\right)$$

$$- \frac{1}{2}\ln N + \frac{5}{4}\ln 2\Big\}. \qquad (23)$$

Substituting N_A, N_B, and N_C by a, b, and c, and ξ_V and kT by $\alpha\xi_V$ and $t\xi_V$, Eq. (22) becomes:

$$\mu_S = \mu_{VS} + \frac{1}{2}g_V + \Big[\frac{3 + \alpha}{2}$$

$$- \frac{1}{4}\Big\{ab + (2 + \alpha)(a + b)c + c^2\Big\}$$

$$+ \frac{1}{8}t\ln(1 - a)(1 - b)(1 - c)^2\Big]\xi_V. \qquad (24)$$

From Eqs. (21) and (24), we obtain:

$$P_{S_2} = Q(t)\exp\Big[\frac{1}{t}\Big\{\frac{3 + \alpha}{2} - \frac{1}{4}\Big\{ab$$

$$+ (2 + \alpha)(a + b)c + c^2\Big\}\Big\}$$

$$+ \frac{1}{8}\ln(1 - a)(1 - b)(1 - c)^2\Big], \qquad (25)$$

where $Q(t) = \frac{1}{2}\exp(\mu_{VS} + \frac{1}{2}g_V)/t$.
It is therefore possible to compute the relationship among the equilibrium sulfur vapor pressure, temperature (t), and the composition, and to compare the derived relationship with experimental data.

3. Results of the Numerical Calculation

3.1. Phase Transition

As an example, the temperature dependence of the equilibrium occupation probabilities a, b, and c for the composition of $x = 1.0$, i.e., $VS_{1.60}$ or the stoichiometric composition of V_5S_8 are shown in Fig. 2 by taking α as a variable. The characteristics of the transitions for this case should be classified into the following three cases.

(1) There is no interaction between partially occupied layers, i.e., $\alpha = 0.0$. The ordered structure of the V_5S_8-type ($a > b \geq c$) directly transforms into the disordered structure of the CdI_2-type ($a = b = c$) at the critical temperature Tc_1, and the occupation probabilities a, b, and c changes discontinuously at Tc_1.

(2) There is small interaction between the partially occupied layers, i.e., $0.0 < \alpha < 0.24$. Only Tc_1 appears, but the transition

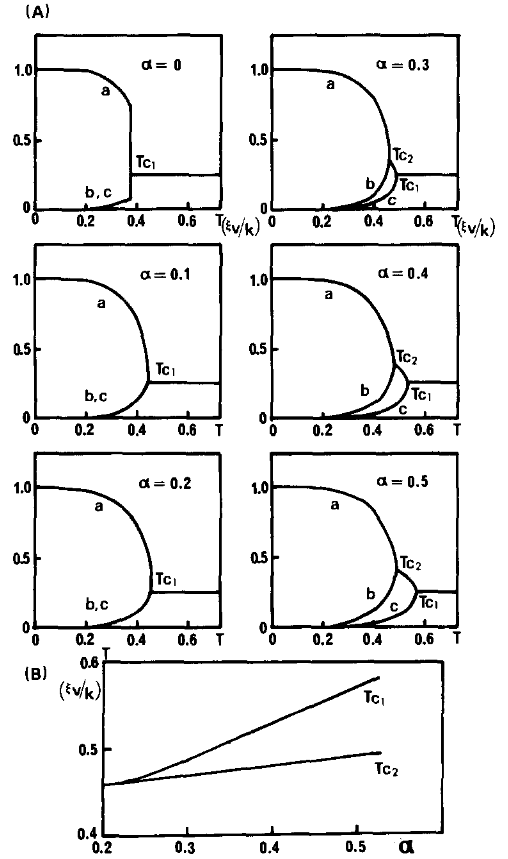

FIG. 2. (A) Occupation probabilities for the composition $VS_{1.60}$ against temperature curves for the change of the value α, which is a ratio of the interlayer ξ_V and the intralayer interaction energy ξ_V. The probabilities a, b, and c are for A, B, and C sites in Fig. 1, respectively. Temperature is measured by ξ_V/k as the unit. Tc_1 and Tc_2 are the transition temperatures corresponding to the transitions of V_3S_4 (or V_5S_8)↔CdI_2 and V_5S_8↔V_3S_4. (B) Tc_1 and Tc_2 vs α curves, derived from (A).

may be of second order, since a, b, and c change continuously at Tc_1.

(3) There is larger interaction, i.e., $\alpha > 0.24$. The V_5S_8-type structure transforms into the V_3S_4-type ($a = b > c$) for the first step at the critical temperature Tc_2. Then the successive transition from the V_3S_4-type to the CdI_2-type occurs at Tc_1. Both transitions may be of second order.

Thus the calculated phase diagram show an interesting feature of the phase transition appearing in the V–S system. By comparing the calculated results with experimental ones for the sample $VS_{1.60}$, it is confirmed that the third case is the most probable one. It is interesting to point out that the phase diagram of the V–S system can be explained only for the case $\alpha > 0.24$, i.e., the interaction energy between partially occupied layers has an important role in the phase transition of the V–S system. A similar calculation has been made for the whole composition range between VS and VS_2. The results obtained are summarized as follows:

(1) Tc_1 has a maximum value at the stoichiometric composition (V_3S_4) and decreases with increase or decrease of sulfur content towards 0°K. The value of Tc_1 increases with increasing α.

(2) Tc_2 has a maximum at the composition slightly more vanadium-rich than stoichiometric V_5S_8, and the maximum value moves toward the sulfur-rich composition with increasing α. At the stoichiometric compositions V_3S_4 and VS_2, Tc_2 becomes 0°K.

(3) The interval between Tc_1 and Tc_2 increases with increasing α. The phase diagram computed with $\alpha = 0.30$ is shown in Fig. 3.

Here we make comparison between the calculated and experimental phase diagrams.

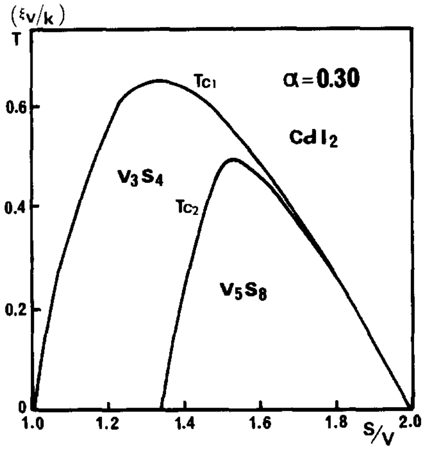

FIG. 3. Phase diagram of the V–S system determined from the numerical calculation using $\alpha = 0.30$.

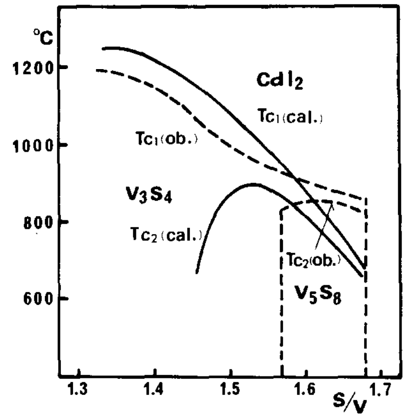

FIG. 4. Calculated and observed phase diagram of the V–S system. Solid lines are the calculated Tc_1 and Tc_2 curves using $\xi_V = 2340$ K and $\alpha = 0.30$. Broken lines are the observed ones from Ref. (*4*). The calculated curves are fitted to the observed ones at the composition $VS_{1.58}$.

Figure 4 shows a comparison of the calculated Tc_1 and Tc_2 values with experimental ones. The calculation was made by taking $\alpha = 0.30$ and $\xi_V = 2340$ K (4.65 kcal/mole), which was obtained by fitting the experimental Tc_1 and Tc_2 to the calculated ones at the composition $VS_{1.58}$.

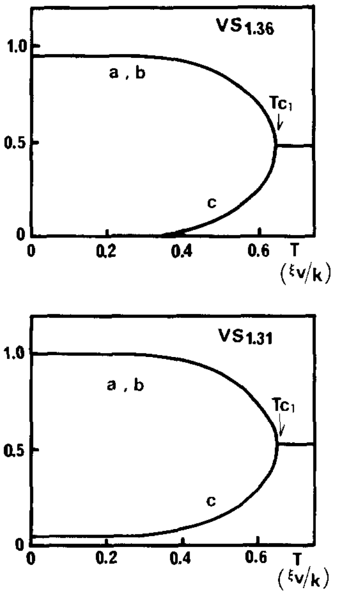

FIG. 5. Occupation probabilities vs temperature curves for $VS_{1.36}$ and $VS_{1.31}$ using $\alpha = 0.30$. Tc_1 indicates the transition temperature from the V_3S_4-type ($a = b > c$) to the CdI_2-type ($a = b = c$).

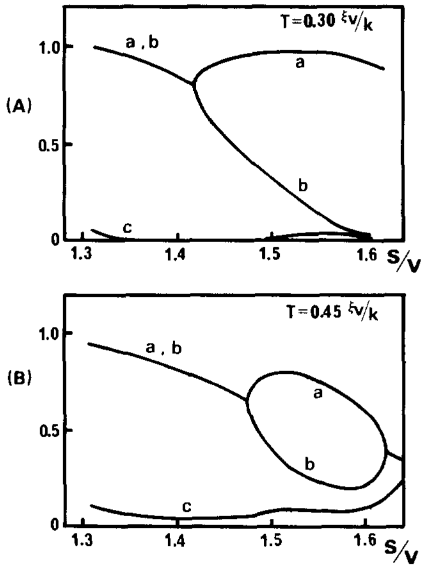

FIG. 6. Occupation probabilities vs composition curves for $T = 0.30$ ξ_V/k (A) and $T = 0.45$ ξ_V/k (B) using $\alpha = 0.30$. The curves for (A) show the transition from the V_3S_4-type ($a = b$) to the V_5S_8-type ($a > b$) at the composition $VS_{1.42}$ and those for (B) show that the V_5S_8 phase exists in the composition range from $VS_{1.47}$ to $VS_{1.62}$.

Next we consider "the order of the phase transition" from the viewpoint of the temperature and composition dependence of the occupation probabilities, and also from the free energy change. As mentioned above, the occupation probabilities *a*, *b*, and *c* for the composition $VS_{1.60}$ show a continuous change with temperature through Tc_2 and Tc_1, which suggests that the phase transitions at Tc_2 and Tc_1 are of second order. In Fig. 5, the temperature dependences of the occupation probabilities are shown for the compositions $VS_{1.31}$ and $VS_{1.36}$, both of which are of the V_3S_4-type structure at room temperature. In Fig. 6, the composition dependences of *a*, *b*, and *c* are shown at temperatures $T = 0.30$ ξ_V/K and $T = 0.45$ ξ_V/K. As seen from both figures, there is no discontinuous change in the temperature or composition vs *a*, *b*, and *c* curves. This again suggests that the phase transition is of second order.

These discussions can be strictly verified by a numerical calculation of the free energy change. Equation (2) can be rearranged as follows:

$$G = G_1 + G_2, \tag{26}$$

where

$$\begin{aligned} G_1 = N\mu_{VS} &+ f_S(N,N_S) \\ &+ \frac{N}{8}(4-x)g_V \\ &+ \frac{N}{4}(2-x)(3\xi_V + \xi'_V), \end{aligned} \tag{27}$$

$$x = a + b + 2c,$$

$$G_2 = \frac{N}{8} f(a,b,c), \tag{28}$$

$$\begin{aligned} f_S(N,N_S) = (N-N_S)g_S &+ \frac{z_S}{2}\frac{(N-N_S)^2}{N}\xi_S \\ &+ kT\{(N-N_S)\ln(N-N_S) \\ &+ N_S \ln N_S - N\ln N\}, \end{aligned} \tag{29}$$

$$\begin{aligned} f(a,b,c) = 2\{ab + 2(a+b)c + c^2\}\xi_V &\\ + (a+b)c\xi'_V + kT\{a\ln a &\\ + (1-a)\ln(1-a) + b\ln b &\\ + (1-b)\ln(1-b) + 2c\ln c &\\ + 2(1-c)\ln(1-c)\}. & \end{aligned} \tag{30}$$

It is evident that the term G_1 depends only on the composition x, while the term G_2 depends on the occupation probabilties. Therefore in order to discuss the order of the phase transitions, it is enough to take only the term $f(a,b,c)$ into consideration. Figure 7a shows the temperature dependence of $f(a,b,c)$ for the composition $VS_{1.60}$ with $\alpha = 0.30$. At temperatures below Tc_2, the free energy for the V_5S_8-type has the lowest energy, and at Tc_2 the curve touches that of the V_2S_4-type with a common tangent, which means that the phase transition from the V_5S_8-type to the

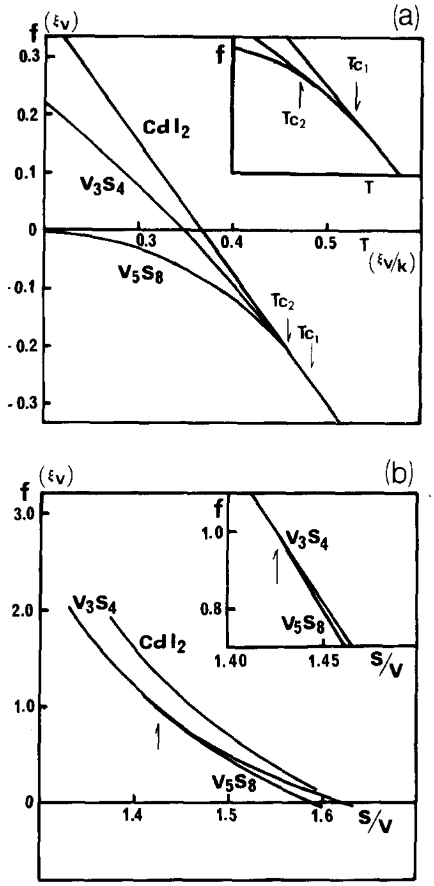

FIG. 7. (a) Free energy $f(a,b,c)$ in Eq. (28) for each type of crystal structure vs temperatlure curves for the composition $VS_{1.60}$ and $\alpha = 0.30$. At Tc_2 (0.462 ξ_V/k) and Tc_1 (0.488 ξ_V/k), the phase transitions occur and the free energy curves touch each other with a common tangent, which shows the transitions to be of second order. The inset shows the detail of the curves near the transition temperatures schematically. (b) Free energy $f(a,b,c)$ in Eq. (28) vs composition curves for the temperature $T = 0.30\ \xi_V/k$ and $\alpha = 0.30$. The transition point is indicated by the arrow. In the inset, the free energy change near the transition point is enlarged to show the transition to be of second order.

V_3S_4-type is of second order. In the temperature range from Tc_2 to Tc_1, the free energy curve for the V_3S_4-type has the lowest energy, and at Tc_1 the curve touches that of the CdI_2-type with a common tangent, which means that the phase transition from the V_3S_4-type to the CdI_2-type is of second order.

The composition dependence of the free energy f at $T=0.30\ \xi_V/K$ is shown in Fig. 7b. At the composition $VS_{1.42}$, the curve for the V_5S_8-type touches that of the V_3S_4-type with a common tangent. This means that the V_3S_4-type structure transforms into the V_5S_8-type at $VS_{1.42}$ and the phase transition is of second order. Thus we can conclude that the order–disorder transitions appearing in the VS–VS_2 system are of second order. These results are consistent with the discussion made by Haas (*12*). Based on the Landau theory of phase transitions, he confirmed that a second-order phase transition is possible in the phase transitions from the V_5S_8-type to the V_3S_4-type and from the V_3S_4-type to the CdI_2-type.

The same treatment has also been made for the V–Se system which shows a behavior similar to that of the V–S system (*4*). This system has slightly lower transition temperatures than the V–S system, which means that ξ_V is smaller than that of the V–S system. Also the interval between Tc_2 and Tc_1 is larger than that of the V–S system, which means that α is larger. As a result, for the V–Se system we take 2035°K or 4.04 kcal/mole for ξ_V and 0.45 for α, deduced from the experimental transition temperatures at $VSe_{1.60}$. In Fig. 8, are shown the calculated curves of Tc_1 and Tc_2 for the V–Se system and also the experimental curves. The agreement with the experimental curves is fairly good.

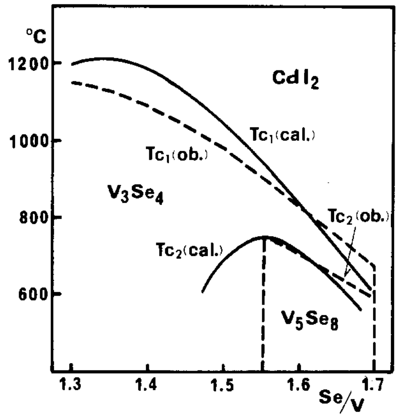

FIG. 8. Calculated and observed phase diagram of the V–Se system. Solid lines are the calculated Tc_1 and Tc_2 curves using $\xi_V = 2035°K$ and $\alpha = 0.45$. Broken lines are the observed ones from Ref. (*4*). The calculated curves are fitted to the observed ones at the composition $VSe_{1.60}$.

3.2. *Equilibrium Sulfur Vapor Pressure*

We tried to calculate the equilibrium sulfur vapor pressure P_{S_2} by Eq. (25), utilizing the numerical calculation of the occupation probabilities a, b, and c. The term $Q(t)$ is unknown. Fortunately, Wakihara *et al.* (*13*) recently measured the P_{S_2} for the composition range from $VS_{1.33}$ to $VS_{1.60}$ at 800°C (*13*). From their data at the composition $VS_{1.404}$ in the temperature range from 650 to 800°C (*14*), we get the temperature dependence of the value $(\mu_{VS} + \frac{1}{2}g_V)$ as shown in Fig. 9. (In this temperature range and low sulfur vapor pressures, S_2 species are predominant in the vapor (*15*, *16*).)

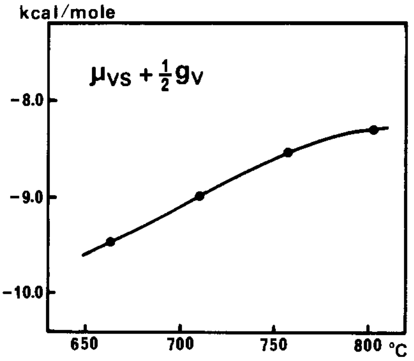

FIG. 9. $\mu_{VS} + \frac{1}{2}g_V$ vs temperature curve. The curve was obtained from Eq. (25) by combining the data of the temperature dependence of the occupation probabilities and vapor pressure (*14*) for $VS_{1.404}$.

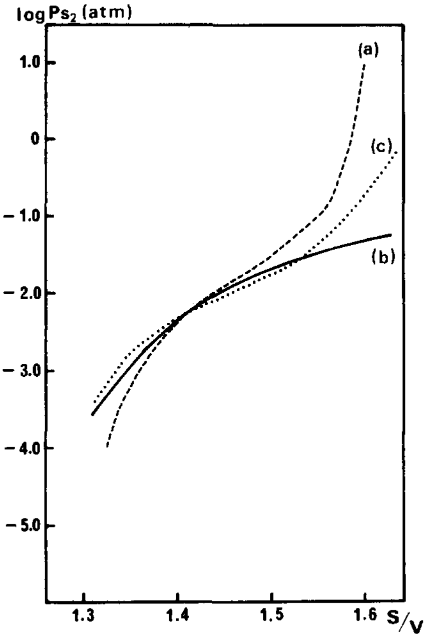

FIG. 10. Calculated and observed sulfur vapor pressure (P_{S_2}) vs composition curves in the V–S system at 800°C. A broken line (a) is the observed P_{S_2} measured by Wakihara *et al.* (*13*) and a solid line (b) is the calculated P_{S_2} obtained from Eq. (25) by fitting the experimental data at the composition $VS_{1.404}$. A dotted line (c) is the recalculated P_{S_2} by using the composition-dependent values of ξ_V in Section 4.

To the first approximation, it is plausible that the value $Q(t)$ does not depend on the composition. Figure 10 shows the calculated P_{S_2} together with the data of Wakihara *et al.* at 800°C. The agreement between the calculated and experimental curves is not so satisfactory, especially in the region of high sulfur content near $VS_{1.60}$. But the tendency of the composition dependence of P_{S_2} should be reproduced in spite of this simple treatment of the equilibrium vapor pressure and more improved calculated curve is given in the next section by assuming the composition dependence of the value ξ_V.

4. Discussion

As mentioned above, the statistical thermodynamic treatment after L and L based on the Bragg–Williams approximation shows qualitative agreement with the experimental facts.

In the case of the order–disorder transition for AB alloys, the pairwise interaction energies between A–A, A–B, and B–B have to be taken into consideration. In our case, therefore the interaction energies between metal–metal, metal–vacancy, and vacancy–vacancy have to be taken into consideration. According to L and L, the interaction energy between metal–metal is implicit in the term $N\mu_{VS}$. By short calculation, the free energy expression (G') including both metal–vacancy and vacancy–vacancy interactions can be obtained as follows:

$$G' = G'_1 + G'_2, \tag{31}$$

$$\begin{aligned} G'_1 = N\mu_{VS} &+ f_S(N, N_S) + (N/8)(4 - x)g_V \\ &+ (N/4)(2 - x)(3\xi_V + \xi'_V) \\ &+ (N/4)x(3\phi_V + \phi'_V), \end{aligned} \tag{32}$$

$$G'_2 = (N/8)f'(a,b,c), \tag{33}$$

$$\begin{aligned} f'(a,b,c) = 2[&\{ab + 2(a + b)c + c^2\}\varepsilon_V \\ &+ (a + b)c\varepsilon'_V] \\ &+ kT\{a \ln a + (1 - a)\ln(1 - a) \\ &+ b \ln b + (1 - b)\ln(1 - b) \\ &+ 2c \ln c + 2(1 - c)\ln(1 - c\}, \end{aligned}$$

where ϕ_V is the intralayer metal–vacancy interaction energy and ϕ'_V is the interlayer one, and $\varepsilon_V = \xi_V - 2\phi_V$, $\varepsilon'_V = \xi'_V - 2\phi'_V$. It is evident that the term G'_1 depends only on the composition x, while the term G'_2 depends on the occupation probabilities. Comparing with Eq. (26), the term G'_2 is formally the same as the term G_2 in Eq. (20). Accordingly, it can be concluded that the free energy expression G gives the same result on the nature of the phase transition as does the expression G'. It is to be noticed that the expression for the chemical potential μ_S is correctly changed into the following relation:

$$\mu_S = \mu_{VS} + \frac{1}{2}g_V + \left[\frac{3+\alpha}{2} - \frac{1}{4}\left\{ab + (2+\alpha')(a+b)c + c^2\right\} + \frac{1}{8}t \ln (1-a)(1-b)(1-c)^2\right]\varepsilon_V + (3+\alpha')\phi_V, \tag{34}$$

where

$$\alpha' = \frac{\varepsilon'_V}{\varepsilon_V} = \frac{\xi'_V - 2\phi'_V}{\xi_V - 2\phi_V}, \quad kT = t\varepsilon_V.$$

We mention here the relation between the treatment of Koiwa and Hirabayashi (*3*) and ours. Koiwa and Hirabayashi discussed the order–disorder transition of oxygen atoms in alpha-titanium (*3*). The free energy expression consists of the interaction energies between interstitial oxygen atoms and configurational entropy of oxygen atoms. According to the treatment of Koiwa and Hirabayashi, the free energy f_k for our case is as follows:

$$\begin{aligned} f_k = {} & 2[\{ab + 2(a+b)c + c^2\}\varepsilon_m \\ & + (a+b)c\varepsilon'_m] + kT\{a \ln a \\ & + (1-a)\ln(1-a) + b \ln b \\ & + (1-b)\ln(1-b) + 2c \ln c \\ & + 2(1-c)\ln(1-c)\}, \end{aligned} \tag{35}$$

where ε_m is the intralayer metal–metal interaction energy and ε'_m is the interlayer one. It is interesting to note that f_k is the same in form to f in Eq. (21) or f' in Eq. (33). To get the free energy minimum, the following conditions must be imposed:

$$\frac{\partial f_k}{\partial a} = 0, \quad \frac{\partial f_k}{\partial b} = 0 \quad (\text{where } a + b + 2c = x\text{: const}), \tag{36}$$

$$\frac{\partial^2 f_k}{\partial a^2} > 0, \quad \frac{\partial^2 f_k}{\partial b^2} > 0, \quad \text{and} \quad \frac{\partial^2 f_k}{\partial a^2} \cdot \frac{\partial^2 f_k}{\partial b^2} - \left(\frac{\partial^2 f_k}{\partial a \partial b}\right)^2 \geq 0.$$

From Eq. (36), the same equations to Eqs. (16) and (17) were obtained. Thus it is clarified that these two methods give the same result on the phase transition. However, the merit of the L and L method is in the following points:

(i) The expression G gives the absolute value of the free energy.

(ii) The equilibrium vapor pressure can be calculated straightforward from G.

Our main purpose is to show that the phase diagram of VS–VS_2 system can be explained by simple statistical thermodynamics. In Section 3, it was confirmed that Eqs. (16) and (17) qualitatively explain the nature of the order-disorder phase transition appearing in the V–S system. In Eqs. (16) and (17), there are adjusting parameters which have to be chosen so as to realize the experimental facts as possible. In Section 3, the calculation was made by taking $\alpha = 0.30$ and $\xi_V = 2340°K$, which was obtained by fitting the values of the experimental Tc_1 and Tc_2 to the calculated ones at the composition $VS_{1.58}$. The results are in rough agreement with the experimental facts. In the calculation, the interaction energies ξ_V and ξ'_V are assumed to be constant over a wide composition range. This assumption seems not to be plausible. For example, we can choose the parameters ξ_V and ξ'_V so as to fit the values of the experimental Tc_1 and Tc_2 to calculated ones over the whole investigated composition range, i.e., ξ_V and ξ'_V are dependent on temperature and composition. The results are shown in Fig. 11. A similar discussion may be plausible for the composition dependence of the equilibrium sulfur vapor pressure at 800°C. By using the composition-dependent values of ξ_V, the P_{S_2} in Eq. (25) was recalculated. Thus the recalculated curve obtained in Fig. 10 is shown by the dotted line. As compared with the curve

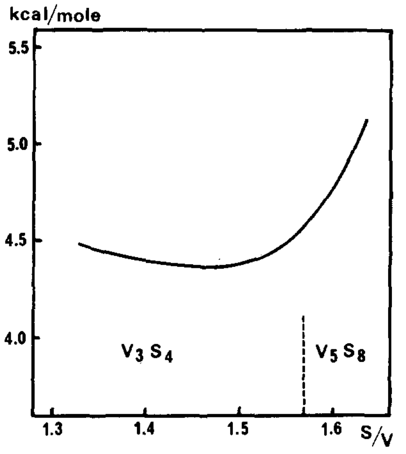

FIG. 11. Composition dependence of the intralayer interaction energy ξ_V. The curve is obtained from the experimental data of the composition dependence of Tc_1 in Ref. (*4*).

obtained by using the constant ξ_V in Subsection 3.2, this curve is in better agreement with the experimental one in the region of high sulfur content near $VS_{1.60}$.

As for the values of $\mu_{VS} + \frac{1}{2}g_V$ (or $\mu_{VS} + \frac{1}{2}g_V + (3 + \alpha')\phi_V$ in Eq. (34)), it is impossible to estimate the vacancy formation energy g_V, because the formation energy for the stoichiometric VS is unknown (stoichiometric VS does not crystallize with the NiAs-type structure but the MnP-type (*17*)). But it is interesting to compare the data with those for the pyrrhotite FeS analyzed by Libowitz (*18*). For example, the values of $\mu_{FeS} + g_{VFe}$ are −12.9 kcal/mole at 670°C and −9.5 kcal/mole at 800°C, and in our case the values of $\mu_{VS} + \frac{1}{2}g_V$ are −9.4 kcal/mole at 670°C and −8.3 kcal/mole at 800°C, as shown in Fig. 9.

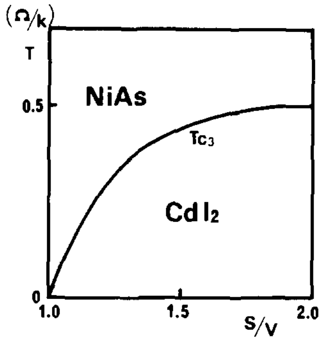

FIG. 12. Composition dependence of the intralayer transition temperature Tc_3 of the V–S system determined from Eq. (37). Temperature is measured by Ω/k in Eq. (37) as the unit. At the transition temperature Tc_3, the CdI_2-type structure transforms into the NiAs-type.

At higher temperatures, the phase transition from the CdI_2-type to the NiAs-type may be expected to appear. But we could not derive the $CdI_2 \leftrightarrow$NiAs transition from Eq. (1), because of the assumption that $d = 1$, i.e., there is no vacancy in the fully occupied layer. In the case of $d \neq 1$, a similar but somewhat complicated expression for the total free energy G is given. From the equation, we can get the phase transition temperature Tc_3 ($CdI_2 \leftrightarrow$NiAs) as follows:

$$Tc_3 = \frac{\Omega}{k}\frac{2}{X}\left(1 - \frac{1}{X}\right), \qquad (37)$$

where X in VS_X, $\Omega = \varepsilon - 3\xi_V$, $\varepsilon = \xi_V'' - \xi_V'$, and ξ_V'' is the interlayer vacancy–vacancy interaction energy between adjacent layers. The composition dependence of the Tc_3 is shown in Fig. 12. For example, the sample $VS_{1.30}$ does not show a phase transition below 1200°C. From this fact combined with Eq. (37), we have:

$$1473°K < Tc_3 = \frac{2}{1.30}\left(1 - \frac{1}{1.30}\right)\frac{\Omega}{k},$$

$$\Omega/k > 4150°K.$$

By using $\xi_V = 2340°K$ and $\alpha = 0.30$ ($\xi_V' = 702°K$), the interlayer interaction energy ξ_V'' is estimated to be more than 11,872°K or 23.6 kcal/mole, which is enormously large compared with the value of ξ_V (= 2340°K). The assumption $d = 1$ adopted in this paper is therefore reasonable in the temperature range in question.

Acknowledgments

The authors wish to express their gratitude to Prof. M. Taniguchi for the use of his experimental sulfur vapor pressure data. Thanks are also due to Mr. M. Kono for the collaboration of the computer program.

References

1. G. G. Libowitz, *J. Solid State Chem.* **1**, 50 (1969), G. G. Libowitz and J. B. Lightstone, *J. Phys. Chem. Solids* **28**, 1145 (1967).
2. J. B. Lightstone and G. G. Libowitz, *J. Phys. Chem. Solids* **30**, 1025 (1969).
3. M. Koiwa and M. Hirabayashi, *J. Phys. Soc. Japan* **27**, 807 (1969).
4. Y. Oka, K. Kosuge, and S. Kachi, *J. Solid State Chem.* **23**, 11 (1978).
5. Y. Oka, K. Kosuge, and S. Kachi, *Phys. Lett. A* **50**, 311 (1974).
6. A. B. de Vries and F. Jellinek, *Rev. Chim. Miner.* **11**, 624 (1974).
7. A. B. de Vries and C. Haas, *J. Phys. Chem. Solids* **34**, 651 (1973).
8. S. Brunie and M. Chevreton, *C. R. Acad. Sci. Paris* **258**, 5847 (1964).
9. I. Kawada, M. Nakano-Onoda, M. Ishii, and M. Nakahira, *J. Solid State Chem.* **15**, 246 (1975).
10. B. G. Silbernagel, R. B. Levy, and F. R. Gamble, *Phys. Rev.* **B11**, 4563 (1975).
11. H. Nishihara, H. Yasuoka, Y. Oka, K. Kosuge, and S. Kachi, *J. Phys. Soc. Japan* **42**, 787 (1977).
12. C. Haas, *Solid State Commun.* **4**, 419 (1966).
13. M. Wakihara, T. Uchida, and M. Taniguchi, *Mater. Res. Bull.* **11**, 973 (1976).
14. M. Taniguchi, private communication.
15. H. Braune, S. Peter, and V. Neveling, *Z. Naturforsch.* **6a**, 32 (1951).
16. D. Detry, J. Dowart, P. Goldfinger, H. Keller, and H. Rickert, *Z. Phys. Chem. N. F.* **55**, 314 (1967).
17. H. F. Franzen and T. J. Burger, *J. Chem. Phys.* **49**, 2268 (1968).
18. G G. Libowitz, "Reactivity of Solids," pp. 107–115, Chapman & Hall, London (1972).